# Point defect structure in CdTe and ZnTe thin films

**V. V. Kosyak · M. M. Kolesnyk · A. S. Opanasyuk**

**Abstract** The point defect structure (PDS) in CdTe and ZnTe thin films grown by the quasi-close volume method on different substrates was investigated. The films were analyzed by X-ray diffraction and scanning electron microscopy. To study the point defects the conductivity–temperature relationships and dark voltage–current characteristics using the theory of space charge limited currents were investigated. The deep energy levels in the band gap (BG) were studied by the method of injection spectroscopy. In the BG of both CdTe and ZnTe a range of trap centers and acceptors with different energy were revealed. To model the PDS in the films the quasi-chemical formalism was applied.

**Keywords** CdTe · ZnTe · Thin films · Quasi-close volume · Point defects · Dark voltage–current characteristic · Injection spectroscopy · Quasi-chemical formalism

## 1 Introduction

The II–VI semiconductors, such as CdTe and ZnTe, have drawn scientists' attention for a long time as perspective materials to produce a wide range of devices for microelectronics. Cadmium telluride single crystals are used as X-ray and gamma radiation detectors, whereas CdTe thin films can be used as base layers in converters of solar energy. The wider band-gap ZnTe is a promising material for green lasers. ZnTe thin films can be used as buffer layers in infrared detectors and solar cells [1, 2].

V. V. Kosyak (✉) · M. M. Kolesnyk · A. S. Opanasyuk
General and Experimental Physics Department,
Sumy State University, Sumy, Ukraine
e-mail: v_kosyak@ukr.net

In order to make electronic equipments of optimal physical properties, it is necessary to produce single-crystals and films with a programmable point defect structure (PDS), as this determines the structure-sensitive properties of the material [2]. The choice of the optimal physical and technological parameters for growth and after-growth processing of the materials, as a rule, is carried out by means of PDS modeling in a semiconductor within the quasi-chemical formalism approach [3]. The procedure of modeling is thus reduced to the solution of a system of equations, which describe interstitial defects in a solid-state from a gas phase, jointly with the full equation of electroneutrality. Quantity and type of the quasi-chemical equations (QE), which describe the PDS equilibrium, depend on the model of defect creation [3–5]. That model is often accepted a priori, because from experimental data it is possible to determine only the type of the dominant point defects at given material processing conditions. In that case the constants of the QE are determined by the optimization multifactor model by comparing the modeled value of charge-free current in samples, with experimental data of high temperature Hall effect measurements. PDS calculation carried out by us [6] with the help of the traditional approach showed that results of modeling have good correlation with experimental data in narrow intervals of technological growth parameters.

Calculation of the concentration of point defects in different materials by "the first principles" approach [7–9] has been proposed recently. It provides the more correct approach to the description of PDS in a material: at first the concentration of the neutral interstitial defects from a gas phase is calculated, and then the processes of their ionization in solid-state depending on the Fermi level position are considered. Thus in [9] the "first-principles" calculation was used to study the annealing process of bulk CdTe.

From our standpoint that approach can be also used for calculating the PDS in II–VI thin films, which condensate in conditions close to equilibrium. So far PDS modeling in thin films with the help of "first-principles" approach has not been carried out.

One more factor that complicates the study of PDS in chalcogenides and the achievement of materials with predetermined characteristics is that researches are not well advanced. Generally authors compared results of modeling of Hall conductivity in CdTe single crystal with experimental data [3, 4]. But the Hall conductivity of a compound semiconductor depends on the concentration of all types of point defects and uncontrolled impurities. In our opinion, as the more correct approach, at first it is necessary to study the structure of native point defects, which are donors, acceptors, or trap centers, and then carry out modeling of PDS, using the so-established parameters of the point defects.

## 2 Experimental

CdTe and ZnTe thin films were grown on glass substrate by the quasi-close volume (QCV) method in vacuum [10]. For sandwich structure production, a metal conducting layer (Mo for CdTe, Cr for ZnTe) was deposited on glass substrate by electron beam evaporation. Injection contacts were made using In, Ag (for CdTe), and Cr, Ni (for ZnTe) by vacuum evaporation. Epitaxial CdTe thin films were also grown on mica substrate.

The compound thin films were grown by using stoichiometric powder of the chalcogenides. The following temperatures were used: evaporation temperature $T_e = 973$ K for ZnTe and $T_e = 893$–$1023$ K for CdTe; substrate temperature $T_s = 323$–$823$ K. The deposition time was $t = 10$–$30$ min.

Surface morphology was investigated by optical and scanning microscopy. To determine the average grain size $d$ in the films we used the Jeffries method. Chemical composition was measured by X-ray spectrometry. The structural analysis was made by X-ray diffraction (XRD) with $CuK_\alpha$ radiation in the $2\theta$ range 20–80°. Phase identification was done by comparison of interplanar distances and relative intensity with standard ASTM data. The lattice spacing was defined by location of $K_{\alpha 1}$ component of the peaks intensity and the Nelson–Riley extrapolation method.

The dark voltage–current characteristic (DVCC) at different temperatures and the (conductivity–temperature) $\sigma$–$T$ relationships in the sandwich samples were measured in vacuum using standard methods. The mechanism of charge transport was determined using the differential method, developed in [11]. That method allows to determinate the mechanisms of charge transport by joint analysis of current density–voltage relationship $j$–$U$, and $\gamma$–$U$, $d(\lg\gamma)/d(\lg U) - U$, where $\gamma = d(\lg j)/d(\lg U)$. In case when DVCC is determined by monopolar injection, the $j$–$U$ relationship is processed by the injection spectroscopy (IS) method in the low and high-temperature approximation [12, 13]. IS method allows to determinate the parameters of the localized centers (LC) in the band gap (BG) by the analysis of DVCC in the mode of space charge limited currents (SCLC). We used the IS method to study LC because most of the existing methods cannot be applied to semi-insulating material like CdTe and ZnTe thin films.

## 3 PDS modeling in CdTe and ZnTe thin films

For the PDS modeling the quasi-chemical formalism was applied. The most general model takes into account the formation of neutral and electrically active defects in the anion ($V_A^0$—vacancy, $A_i^0$—interstitial atom) and cation ($V_B^0$—vacancy, $B_i^0$—interstitial atom) sublattices, as well as the existence of antistructural defect $B_A^0$. The antistructural defect $A_B^0$ was not taken into account, as its existence in our materials is improbable [8, 9].

In full equilibrium conditions, the concentration of any point defect can be expressed through thermodynamic potentials of defect creation process, by the law of mass action [5]:

$$N(V_A^0) = \frac{n_0}{P_A} K \exp\left(\frac{S_{V_A^0}^{vib}}{k}\right) \exp\left(-\frac{E_{V_A^0} + U_{V_A^0}^{vib}}{kT}\right), \quad (1)$$

$$N(A_i^0) = P_A n_0 K \exp\left(\frac{S_{A_i^0}^{vib}}{k}\right) \exp\left(-\frac{E_{A_i^0} + U_{A_i^0}^{vib}}{kT}\right), \quad (2)$$

$$N(V_B^0) = P_A n_0 K \exp\left(\frac{S_{V_B^0}^{vib}}{k}\right) \exp\left(-\frac{E_{V_B^0} + U_{V_B^0}^{vib}}{kT}\right), \quad (3)$$

$$N(B_i^0) = \frac{n_0}{P_A} K \exp\left(\frac{S_{B_i^0}^{vib}}{k}\right) \exp\left(-\frac{E_{B_i^0} + U_{B_i^0}^{vib}}{kT}\right), \quad (4)$$

$$N(B_A^0) = \frac{n_0}{P_A^2} K^2 \exp\left(\frac{S_{B_A^0}^{vib}}{k}\right) \exp\left(-\frac{E_{B_A^0} + U_{B_A^0}^{vib}}{kT}\right), \quad (5)$$

where $K = (2\pi m)^{3/2} \frac{(kT)^{5/2}}{h^3}$; $h$ is Planck constant, $T$ the temperature, $k$ the Boltzman constant, $m$ the mass of particle, $P_A$ the pressure of metal vapor, $n_0$ the concentration of lattice sites; $E_X$ the energy of defect creation (X = A, V, B); $U_X^{vib}$, $S_X^{vib}$ the vibrational energy and entropy.

Besides for calculation of $P_A$ at the substrate, gas dissociation, and transport phenomena, that are typical for evaporation of a material in QCV system [14], were also taken into account.

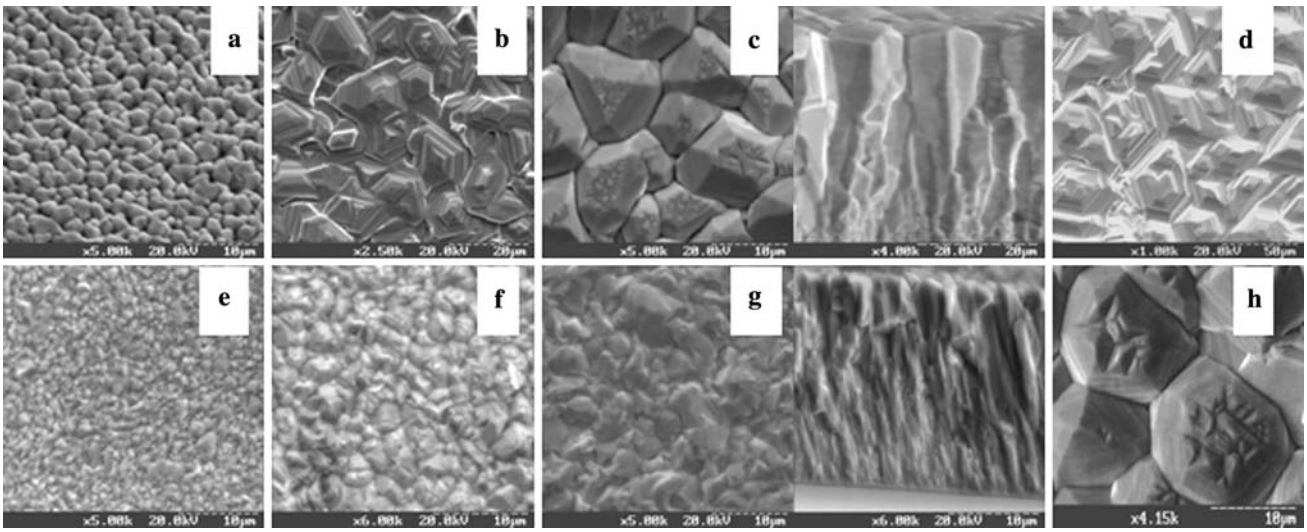


**Fig. 1** A surface and cross-section SEM images of the CdTe:Mo: $T_e = 923$ K; (**a**) $T_s = 573$ K; (**b**) $T_s = 803$ K; (**c**) $T_s = 783$ K with cross-section; (**d**) CdTe: mica $T_s = 833$ K; and of the ZnTe:Cr: $T_e = 973$ K; (**e**) $T_s = 573$ K; (**f**) $T_s = 603$ K; (**g**) $T_s = 693$ K with cross-section; (**h**) $T_s = 823$ K

**Fig. 2** XRD data for the same samples as in Fig. 1

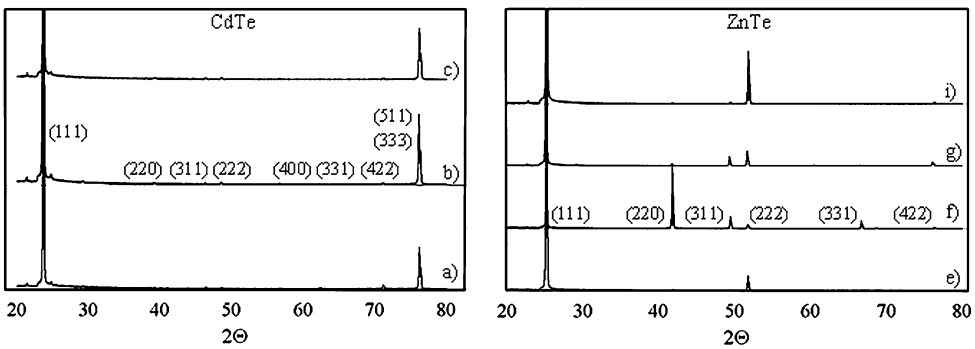


The values of $E_X$, $U_X^{vib}$, $S_X^{vib}$ in Eqs. 1–5 are determined "ab initio", i.e., from the quantum-mechanical and thermodynamical parameters of *Cd*, *Zn*, and *Te* atoms. But at present time this method is rather inaccurate and therefore there exist essential differences in the value of thermodynamic functions determined by the different authors [8, 9, 15, 16]. In particular, conflicting data exist for the value of the formation energy of the antistructural defect $Te_{Cd}^0$ and tellurium vacancy $V_{Te}^0$. Therefore, in our opinion, the most certain results of calculation of thermodynamic functions of defect creation process are those which have found sufficient agreement with experiment data, i.e., the $E_X$, $U_X^{vib}$, $S_X^{vib}$ values given in [5] for the bulk crystals. We used them also for modeling PDS in CdTe and ZnTe thin films. As the thermodynamic functions of defect creation for some point defects are indeterminate, we calculated PDS in ZnTe thin films only partially, i.e., for the dominant native defects.

If the concentrations of neutral defects are determined, it is easy to find the concentration of donor and acceptor charged point defects with use of the Fermi-Dirac statistics and equation of electro-neutrality:

$$n = \frac{N_c}{\exp\left[(E_g - \mu_F)/kT\right] + 1}, \tag{6}$$

$$p = \frac{N_v}{\exp\left(\mu_F/kT\right) + 1}, \tag{7}$$

$$N(X_{di}^{z+}) = \frac{N(X_{di}^0)}{g_d \exp\left[-(E_g - \Delta E_{di} - \mu_F)/kT\right] + 1}, \tag{8}$$

$$N(X_{ai}^{z-}) = \frac{N(X_{ai}^0)}{g_a \exp\left[(\Delta E_{ai} - \mu_F)/kT\right] + 1}, \tag{9}$$

$$\begin{aligned} n + N(V_A^-) + 2N(V_A^{2-}) + N(B_i^-) + 2N(B_i^{2-}) \\ = p + N(A_i^+) + 2N(A_i^{2+}) + N(V_B^+) + 2N(V_B^{2+}) \\ + N(B_A^+) + 2N(B_A^{2+}), \end{aligned} \tag{10}$$

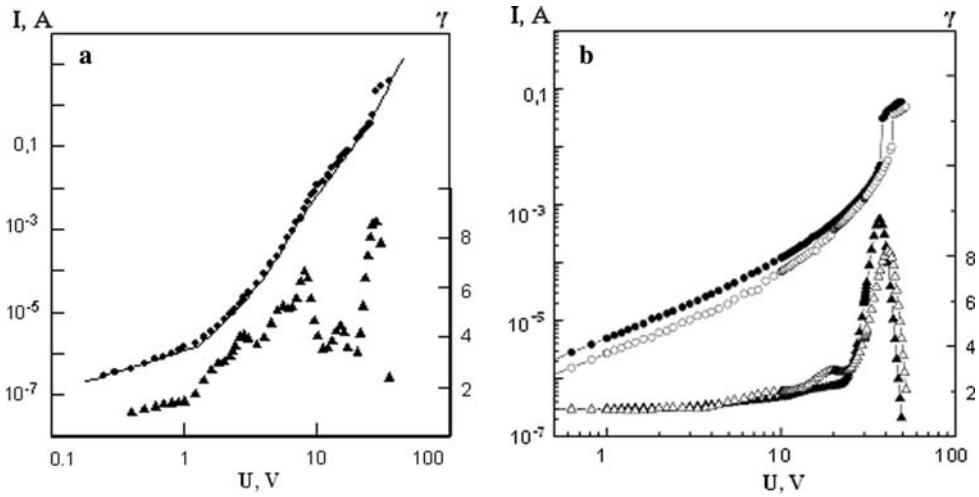


**Fig. 3** DVCC SCLC and differential curve for : (**a**) Ag-CdTe:Mo: ●—$I(U)$; ▲—$\gamma$ $(U)$; (**b**) Ni-ZnTe:Cr: ●—anode on Ni contact, ○—anode on Cr contact—$I(U)$; ▲, Δ: corresponding $\gamma$ $(U)$

**Table 1** Parameters of LC determined in CdTe thin films by high temperature IS method

| Samples number | $L$ (μm) | $T_s$ (K) | $T_e$ (K) | $\Delta E$ (eV) | $\sigma_0$ (eV) | $N$ (cm$^{-3}$) |
|---|---|---|---|---|---|---|
| 1 Polycrystalline | 8 | 743 | 1023 | 0.63 | 0.030 | $4.4 \cdot 10^{13}$ |
| 2 Polycrystalline (first measurement) | 19 | 748 | 948 | 0.61 | 0.031 | $1.7 \cdot 10^{13}$ |
| | | | | 0.45 | 0.028 | $7.3 \cdot 10^{13}$ |
| 2 Polycrystalline (second measurement) | 19 | 748 | 948 | 0.62 | 0.035 | $1.5 \cdot 10^{13}$ |
| | | | | 0.45 | 0.032 | $8.1 \cdot 10^{13}$ |
| 3 Polycrystalline | 12 | 748 | 968 | 0.68 | 0.023 | $7.8 \cdot 10^{12}$ |
| | | | | 0.62 | 0.023 | $1.5 \cdot 10^{13}$ |
| | | | | 0.53 | 0.027 | $6.1 \cdot 10^{13}$ |
| 4 Epitaxial | 11 | 753 | 933 | 0.62 | 0.019 | $4.6 \cdot 10^{12}$ |
| | | | | 0.52 | 0.009 | $1.3 \cdot 10^{13}$ |
| | | | | 0.41 | 0.016 | $1.1 \cdot 10^{14}$ |
| 5 Polycrystalline | 15 | 753 | 953 | 0.60 | 0.019 | $2.3 \cdot 10^{12}$ |
| | | | | 0.52 | 0.020 | $3.6 \cdot 10^{12}$ |
| | | | | 0.46 | 0.020 | $8.6 \cdot 10^{12}$ |
| | | | | 0.41 | 0.015 | $1.4 \cdot 10^{13}$ |
| 6 Polycrystalline | 26 | 758 | 978 | 0.61 | 0.023 | $3.6 \cdot 10^{12}$ |
| | | | | 0.56 | 0.015 | $3.0 \cdot 10^{13}$ |
| | | | | 0.52 | 0.015 | $7.4 \cdot 10^{13}$ |

with $N_{c(v)} = 2\left(\frac{2\pi m_{e(p)} kT}{h^2}\right)^{3/2}$ the effective density of states in the conduction (valence) band, $n$ and $p$ the electron and hole concentration, respectively, $m_{e(p)}$ the electron or hole effective mass, $E_g$ the BG energy, $\mu_F$ the Fermi energy, $z$ the degree of defect ionization, $g$ the degeneracy factor, $\Delta E_{ai}$ and $\Delta E_{di}$ the acceptor and donor ionization energies, $N(X^0)$ the concentration of neutral defects, $N(X_{di}^{z+})$ the donor concentration, $N(X_{ai}^{z-})$ the acceptor concentration.

The acceptor ionization energies and position of Fermi level are calculated from the valence band top, those of donors from the conduction band bottom. As factors of spin degeneracy of the levels we used $g = 2$ for singly charged donor defects and $g = 1/2$ for acceptor levels and for doubly charged centers according to [5].

The acceptor and donor ionization energies in CdTe and ZnTe are taken from [3–5, 9, 16–18] and from our experimental investigation.

## 4 Results

Our chalcogenides thin films have single-phase (zinc-blend) polycrystalline structure in a wide range of growth temperature. The structural properties of the films depended on the growth mechanism. The layers first grow on the substrate with a fine-grained structure with (111) oriented crystallites. Subsequent crystallite growth depends of the temperature. At low substrate temperatures

**Table 2** Interpretation of LC and comparison with results of modeling

| $E_c - \Delta E$ or $E_v + \Delta E$ (eV) | | | Supposed interpretation | Growth condition | $N$ ($cm^{-3}$) | |
|---|---|---|---|---|---|---|
| From DVCC SCLC | From $\sigma$–$T$ dependences | | | | From DVCC SCLC | From PDS modeling |
| Polycrystalline films | Polycrystalline films | Epitaxial films | | | | |
| CdTe | | | | | | |
| $E_c - 0.70$ | $E_c - 0.80$ | – | $V_{Te}^{2+}$ ($E_c - 0.71$) [15] | $T_s = 748$ K<br>$T_e = 933$ K | $1.1 \cdot 10^{14}$ | $8.4 \cdot 10^{13}$ |
| | | | | $T_s = 748$ K<br>$T_e = 953$ K | $1.4 \cdot 10^{14}$ | $8.1 \cdot 10^{13}$ |
| $E_c - 0.61$ | $E_c - 0.60$ | – | $Te_{Cd}^{2+}$ ($E_c - 0.59$) [15] | – | – | – |
| $E_c - 0.56$ | $E_c - 0.57$ | – | $Cd_{ic}^{2+}$($E_c - 0.56$) [15] | – | – | – |
| $E_c - 0.52$ | – | – | – | – | – | – |
| $E_c - 0.46$ | $E_c - 0.46$ | $E_c - 0.46$ | $Cd_{ic}^{+}$ ($E_c - 0.46$) [15] | $T_s = 748$ K<br>$T_e = 933$ K | $7.3 \cdot 10^{13}$ | $7.8 \cdot 10^{13}$ |
| | | | | $T_s = 748$ K<br>$T_e = 953$ K | $8.6 \cdot 10^{12}$ | $7 \cdot 10^{13}$ |
| | | | | $T_s = 748$ K<br>$T_e = 968$ K | $8.1 \cdot 10^{12}$ | $8.8 \cdot 10^{12}$ |
| $E_c - 0.40$ | $E_c - 0.41$ | $E_c - 0.40$ | $V_{Te}^{+}$ ($E_c - 0.40$) [9]<br>$Te_{Cd}^{2+}$ ($E_c - 0.40$) [9] | – | – | – |
| – | – | $E_c - 0.29$ | $Cd_{ia}^{+}$ ($E_c - 0.33$) [15] | – | – | – |
| – | – | $E_c - 0.23$ | $Cd_{ia}^{2+}$ ($E_c - 0.20$) [9] | – | – | – |
| – | $E_v + 0.15$ | $E_v + 0.14$ | $V_{Cd}^{-}$ ($E_v + 0.13$) [15] | – | – | – |
| | – | $E_v + 0.07$ | – | – | – | – |
| ZnTe | | | | | | |
| – | $E_v + 0.72$ | – | $O_{Te}$ | – | – | – |
| $E_v + 0.58$ | $E_v + 0.56$ | – | $V_{Te}^{+}$ [18] | – | – | – |
| – | $E_v + 0.42$ | – | $V_{Zn}^{2-}$ [18] | – | – | – |
| $E_v + 0.21$ | – | – | $V_{Zn}^{-}$ [18] | – | – | – |

There are two interstitial sites in zinc-blende structure: cations (c) $Cd_{ic}$, anions (a) $Cd_{ia}$

of $T_s < 450$–$500$ K (for CdTe), i.e., with high coefficient of vapor supersaturation, almost no increase of crystallite size occurred and the crystallite shape was close to equiaxial. At high substrate temperatures the mechanism of growth changed, and thin films had columnar structure.

The columnar grain diameter depended on the parameters of condensation in the QCV growth run and thickness L of thin films (Fig. 1). At high temperature the grain size increases from $d = 0$, 1 to 5–8 μm at $L \sim 10$ μm. Under identical growth conditions the grain size in CdTe thin films was bigger than in ZnTe.

X-ray diffraction data (Fig. 2) showed that the chalcogenide layers had a [111] axial growth texture, their perfection increased with thickness and depended on substrate temperature.

Experimentally determined value of the lattice constant for CdTe was $a = 0.64810$–$0.64820$ nm and for ZnTe $a = 0.60990$–$0.61200$ nm being in good correlation with ASTM data ($a_{CdTe} = 0.64820$ nm, $a_{ZnTe} = 0.61026$ nm). As the ASTM data correspond to stoichiometric material, then the fact that our lattice constants are very close to the ASTM ones indicates small deviation from stoichiometry in our films. This is also confirmed by X-ray spectrometry analysis.

The CdTe layers have $n$- or $p$-type conductivity, ZnTe only $p$-type conductivity. The films resistivity was $\rho = 5 \cdot 10^6$–$10^{11}$ Ω cm ($n_0 = 2.1 \cdot 10^{10}$–$4.2 \cdot 10^{14}$ $cm^{-3}$), and epitaxial thin films have resistivity 1–2 orders of magnitude smaller than polycrystalline samples.

The DVCC of sandwich structures of chalcogenide thin films, with columnar structure, obtained at $T_s >$ 500–600 K was non-linear. Due to high boundary resistivity the charge transport was, generally, through the grains volume [19, 20]. And analysis has shown that the form of the DVCC was determined only by monopolar injection from the current-collecting contact.

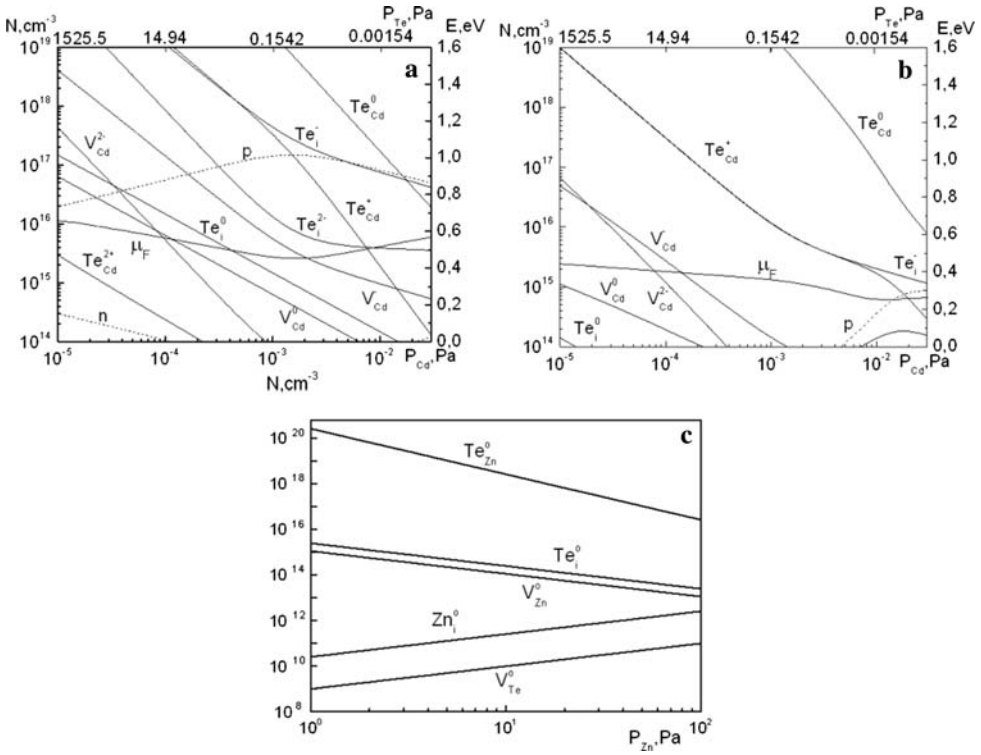


**Fig. 4** Concentration of native point defects and Fermi energy as a function of the partial pressure of cadmium vapor: (**a**, **b**) CdTe thin films, full equilibrium ($T_s = 823$ K, $T_e = 823$–$923$ K), and quenching ($T_s = 293$ K), respectively; (**c**) neutral point defect concentrations in ZnTe thin films as a function of the partial pressure of zinc vapor ($T_s = 823$ K)

Typical DVCCs in the mode of SCLC are shown in Fig. 3. By extracting the $\gamma - U$ dependence from the DVCC curves it is possible to disclose their fine structure. Usually one finds at maximum four super-linear parts each of them conditioned by the filling of the deep traps by injected carriers. The DVCCs are then processed by the low and high temperature approximation of the IS method in the mode of SCLC [13]. In so doing we got the distribution of trap concentrations in the BG $h(E) - E$ (where $h(E) = dN/dE$) and determined their depth ($\Delta E$) in the BG and concentration ($N$). $\Delta E$ were calculated by location of the maximums on the $h(E)$ curves and $N$ by the area under curves. The accuracy of the determination of traps energy level by this method was $kT$ (0.026 eV at room temperature), and for LC concentration did not exceed 30%.

We have seen that in CdTe polycrystalline thin films typically a range of $h(E)$ distributions close to the Gaussian distribution $\left(h(E) = \frac{N}{\sigma_0(2\pi)^{1/2}} \exp\left(-\frac{\Delta E^2}{2\sigma_0^2}\right)\right)$ with half-width $\sigma_0$ exists in the BG. Tailing of trap energy levels can be explained by the existence of fluctuation irregularities of crystal lattice in the layers near the substrate.

The results of calculation of deep traps parameters in CdTe are given in Table 1. We determined LC with $\Delta E_1 = 0.68$ eV; $\Delta E_2 = 0.61$ eV; $\Delta E_3 = 0.56$ eV; $\Delta E_4 = 0.52$ eV; $\Delta E_5 = 0.46$ eV; $\Delta E_6 = 0.40$ eV and concentration $N$ in the range $10^{12}$–$10^{14}$ cm$^{-3}$.

The LC-spectrum in ZnTe BG was less informative than in CdTe: generally the measured traps were close to monoenergy with $\Delta E = 0.21$ or $\Delta E = 0.58$ eV and concentration $N = 10^{14}$–$10^{15}$ cm$^{-3}$.

The point defect ionization energy was also determined from the conductivity–temperature ($\lg\sigma - 1/T$) relationships by standard methods. Such relationships had the traditional shape for semiconductors and are not shown in this article. In the case of CdTe thin films 2–5 linear sections were observed. $\Delta E$ was determined by the curve slope. These investigations have good correlation with values of trap energy levels calculated by IS and presented in Table 2. In case of ZnTe three linear sections were observed on the $\lg\sigma - 1/T$ plots with activation energy $\Delta E_1 = 0.42$, $\Delta E_2 = 0.56$, and $\Delta E_3 = 0.72$ eV.

As the chalcogenide films were not doped and measurements carried out in layers with imperfections at substrate interface, the wide spectrum of traps corresponds to native defects and their complexes with uncontrolled impurities. In case of CdTe the supposed concentration of uncontrolled impurities is $N \approx 10^{14}$–$10^{15}$ cm$^{-3}$, which exceeds the sensitivity of the IS method.

Presently the spectrum of energy levels of point defects in the cadmium telluride BG is not enough studied and the identification of the majority of them is disputable. In the review [17], reporting on the recent results on the determination of depth $\Delta E$ of LCs of different nature, more than 150 deep energy levels are given as determined by the method of current photo-induction only. Most of them are caused just by native point defects. The possibility to unequivocally determine the energy $\Delta E$ of native defects is

given by the theoretical work [8, 9, 15, 16], whereby such energy can be established from "first principles" calculations.

By first calculating the concentration of neutral point defects by Eqs. 1–5, and later solving the system of Eqs. 6–10 we get the dependence of the Fermi level and of the concentration of point defects on the thin film growth parameters. The obtained results and their comparison with those of the PDS modeling are given in Table 2.

The results of the calculation of point defect concentrations as a function of metal partial pressure for the two extreme cases of full equilibrium and quenching are shown in Fig. 4.

The quenching case is more correct for comparison between experiment and results of modeling as the cooling after growth is rather fast. According to Fig. 4 the concentration of free carriers does not exceed $10^{15}$ $cm^{-3}$ and thin films were highly resistive. This was confirmed by experimental investigations.

Presently, experimental data on the nature and energetic location of levels associated with native point defects in ZnTe and CdTe are rather ambiguous. Therefore, interpretation of LC is based on "first principles" calculation data [9, 15, 16]. Unfortunately, since these methods are rather inexact, this does not allow interpreting our results unambiguously.

## 5 Conclusion

By analysis of DVCC in the SCLC mode and conductivity–temperature relationships PDS in CdTe and ZnTe thin films with certified structural characteristics were investigated. The depth in the BG of native point defects and complexes of native defects-impurities and their concentration under different growth conditions were determined. Their interpretation was carried out according to literature data.

The PDS in the thin films was modeled, for full equilibrium and quenching cases, by using the most general model of defect creation. Comparison between the experimental data and results of modeling was performed not only for the free carrier concentration by the traditional approach but also for the concentrations of every native point defect. Good correlation between experimental data and results of modeling was observed.

## References


1. R. Bhargava, *Properties of Wide Band Gap II–VI Semiconductors* (The Institution of Electrical Engineers, London, 1997), p. 238
2. X. Wu, Solar Energy **77**(6), 803 (2004)
3. F. Kreger, *The Chemistry of Imperfect Crystals* (North-Holland, Amsterdam, 1964), p. 654
4. S. Chern, F. Kreger, J. Solid State Chem. **14**, 33 (1975)
5. R. Grill, A. Zappettini, Prog. Cryst. Growth Charact. Mater. **48**, 209 (2004)
6. V.V. Kosyak, A.S. Opanasyuk, Funct. Mater. **12**, 797 (2005)
7. M.A. Berding, M. Schilfgaarde, Phys. Rev. B. **50**, 1519 (1994)
8. M.A. Berding, M. Schilfgaarde, J. Vac. Sci. Technol. **A8**, 1103 (1990)
9. M.A. Berding, Phys. Rev. B. **60**, 8943 (1999)
10. J. Luschitz, K. Lakus-Wollny, Thin Solid Films (in press)
11. P. Olecseenko, G. Sukach, Semicond. Phys. Quantum Electron. Optoelectron. **1**, 112 (1998)
12. S. Nespurek, J. Sworakowski, J. Mol. Electr. **5**, 71 (1989)
13. A. Opanasyuk, N. Opanasyuk, Semicond. Phys. Quantum Electron. Optoelectron. **6**, 444 (2003)
14. V.V. Kosyak, M.M. Kolesnik, Radiat. Meas. **42**, 855 (2007)
15. S.H. Wei, S.B. Zhang, Phys. Rev. B. **66**, 155211 (2002)
16. E. Erbarut, Sold State Commun. **128**, 113 (2003)
17. X. Mathew, Solar Energy Mater. Solar Cells **76**, 225 (2003)
18. Yu.G. Sadofyev, M.V. Korshkov, Semicond. Phys. Technol. **35**, 525 (2002)
19. W. Huber, A. Lopez-Otero, Thin Solid Films **58**, 21 (1979)
20. T. Thorpe, A. Fahrenbruch, J. Appl. Phys. **60**, 3622 (1986)